Available online at www.sciencedirect.com
SCIENCE DIRECT®
Journal of Solid State Chemistry 179 (2006) 2298–2309
JOURNAL OF SOLID STATE CHEMISTRY
www.elsevier.com/locate/jssc

$M_{1-x}[W_2O_2X_6]$ with $M = K^+$, Tl^+, Ag^+, Hg^{2+}, Pb^{2+}; $X = Cl$, Br—A class of mixed valence tungsten (IV,V) compounds with layered structures, W–W bonds and high conductivity

Johannes Beck[a,*], Christian Kusterer[a], Rolf-Dieter Hoffmann[b,1], Rainer Pöttgen[b,1]

[a]*Institut für Anorganische Chemie, Rheinische Friedrich-Wilhelms-Universität, Gerhard-Domagk-Straße 1, D-53121 Bonn, Germany*
[b]*Institut für Anorganische und Analytische Chemie, Westfälische Wilhelms-Universität, D-48149 Münster, Germany*

Received 23 January 2006; received in revised form 31 March 2006; accepted 2 April 2006
Available online 15 May 2006

Dedicated to Prof. Hans Georg von Schnering on the occasion of his 75th birthday

Abstract

The crystal structure of $WOCl_3$, determined on the basis of powder diffraction data (tetragonal, $P4_2/mnm$, $a = 10.6856(6)$, $c = 3.8537(2)$), is isotypic to WOI_3 and contains one-dimensional strands of edge-sharing double-octahedral $W_2O_{4/2}Cl_6$ groups connected via common corners in trans position. A W–W bond of 2.99 Å is present within the planar W_2Cl_6 groups. A series of non-stochiometric, mixed valence W(IV,V) compounds $M_{1-x}[W_2O_2Cl_6]$ can be obtained from $WOCl_3$ by reaction with metal halides (TlCl, KCl, $PbCl_2$) or by reaction of elemental Hg with $WOCl_4$. All were characterized by single crystal structure determinations and EDX measurements ($Tl_{0.981(2)}[W_2O_2Cl_6]$: monoclinic, $C2/m$, $a = 12.7050(4)$, $b = 3.7797(1)$, $c = 10.5651(3)$ Å, $\beta = 107.656(1)^\circ$; $K_{0.84(2)}[W_2O_2Cl_6]$: monoclinic, $C2/m$, $a = 12.812(3)$, $b = 3.7779(6)$, $c = 10.196(3)$ Å, $\beta = 107.422(8)^\circ$; $Pb_{0.549(3)}[W_2O_2Cl_6]$: orthorhombic, $Immm$, $a = 3.7659(1)$, $b = 9.8975(4)$, $c = 12.1332(6)$ Å; $Hg_{0.554(6)}[W_2O_2Cl_6]$: monoclinic, $C2/m$, $a = 12.8361(8)$, $b = 3.7622(3)$, $c = 10.2581(9)$ Å, $\beta = 113.645(3)^\circ$). Two representatives of this family of compounds have already been reported: $Na[W_2O_2Br_6]$ [Y.-Q. Zhang, K. Peters, H.G. von Schnering, Z. Anorg. Allg. Chem. 624 (1998) 1415–1418] and $Ag_{0.74}[W_2O_2Br_6]$ [S. Imhaïne, C. Perrin, M. Sergent, Mat. Res. Bull. 33 (1998) 927–933]. The Ag containing compound can be obtained from elemental Ag and $WOBr_3$. The crystal structure, originally reported in the triclinic system, was redetermined and shown to be monoclinic with space group $C2/m$ ($a = 13.7338(10)$, $b = 3.7769(3)$, $c = 10.7954(9)$ Å, $\beta = 112.401(3)^\circ$). The crystal structures of these compounds are in close relationship to the structure of $WOCl_3$ and all contain $W_2O_{4/2}X_6$ (X = Cl, Br) double strands with the mono and divalent cations coordinated by the terminal halogen atoms of the W_2X_6 groups and a short W–W bond (2.85 Å for X = Cl). A cube-shaped coordination environment is present for M = Tl, K and a trigonal-prismatic coordination for M = Ag, Hg. $Hg_{0.55}[W_2O_2Cl_6]$ is a semiconductor with a non-Arrhenius behaviour, high specific conductivity of $0.05\,\Omega^{-1}\,cm^{-1}$ and a very small activation energy of 0.03 eV. $Hg_{0.55}[W_2O_2Cl_6]$ and $Ag_{0.8}[W_2O_2Br_6]$ show a temperature independent paramagnetism with a magnetic moment around $300 \times 10^{-6}\,cm^3\,mol^{-1}$.

Keywords: Tungsten oxide chloride; Mixed valence compounds; One-dimensional structures; Non-stoichiometric compounds; Magnetic properties; Conductivity

1. Introduction

In 1959, Sands et al. provided a single crystal structure determination of the structure of $NbOCl_3$, which became the aristotype of the MOX_3 (M = transition metal, X = halogen) structure family: pairs of NbO_2Cl_4 octahedra, edge shared via chlorine bridges, are connected via equidistant –O–Nb–O– bridges to form one dimensional double-strands $^{\infty}_{1}[Nb_2O_{4/2}Cl_4Cl_{2/2}]$ [1]. Since the structure was described in the centrosymmetric space group $P4_2/mnm$, the Nb atoms had to be placed in the mirror plane perpendicular to the c-axis together with the chlorine

*Corresponding author. Fax: +49 228 735660.
E-mail address: j.beck@uni-bonn.de (J. Beck).
[1]Investigation of magnetic properties.

0022-4596/$ - see front matter © 2006 Elsevier Inc. All rights reserved.
doi:10.1016/j.jssc.2006.04.006

atoms, leading to planar $Nb_2Cl_4Cl_{2/2}$ groups. The Nb–Nb distance was found to be 3.91 Å. The space group $P4_2/mnm$ was also assumed by Drew and Tomkins for the structure of $MoOBr_3$, but they found it necessary to split the Mo atom site in two closely neighboured positions above and below the mirror plane [2]. The Mo–Mo distance was found to be 3.86 Å and thus outside of the range of Mo–Mo bonds. Magnetic measurements showed the compound to be paramagnetic with a moment corresponding to Mo(V). In 2002, Ströbele and Meyer succeeded in the redetermination of the crystal structure of $NbOCl_3$, which revealed the non-centrosymmetric space group $P\bar{4}2_1m$. They found the $^{\infty}_{1}[Nb_2O_{4/2}Cl_4Cl_{2/2}]$ strands to be polar with asymmetric –O···Nb–O··· bridges and the Nb atoms shifted out of the plane of the surrounding Cl atoms [3]. The non-centrosymmetry of the structure was confirmed independently by a second harmonic generation experiment [4]. The undistorted, higher symmetric structure type was meanwhile found for WOI_3 which in fact exhibits planar W_2I_6 units and equidistant, almost linear –O–W–O– bridges [5]. In contrast to $NbOCl_3$ and $MoOBr_3$, a much shorter W–W distance of 3.10 Å is present in the structure. The magnetic moment of WOI_3 is very low (0.24 B.M. at 583 K), probably due to spin coupling between the neighboured W atoms. In other words, a bond seems to exist between the two tungsten atoms over the edge of each two fused WO_2I_4 octahedra. The structure of $WOCl_3$ was not known in detail up to now, but since a low magnetic moment was measured [6], a W–W bond can be expected to be present in its structure.

Tungsten oxide trihalides WOX_3 can act as Lewis acids towards halide ions. Under addition of X^- the $^{\infty}_{1}[W_2O_{4/2}X_4X_{2/2}]$ double strands brake off to yield negatively charged polar $^{\infty}_{1}[WO_{2/2}X_4]^-$ single strands, which are structurally related to the respective W(VI) oxide tetrahalides WOX_4. As counterions in structures with single strands only large polycationic clusters like Te_7^{2+} or Te_6^{2+} are known as found in the structures of $Te_7[WOBr_4]Br$ [7] and $Te_6[WOCl_4]_2$ [8]. This stands in contrast to the reactivity of the respective niobium oxide trihalides $NbOX_3$ which form adducts with halides of monoatomic cations. Examples are $Tl[NbOX_4]$ (X = Cl, Br), both containing polar single strands $^{\infty}_{1}[NbO_{2/2}X_4]^-$ [4]. Another type of reactivity of WOX_3 is the reduction to compounds of the general formula $M[W_2O_2X_6]$ (X = Cl, Br). Only two representatives have been reported until today, both in 1998 by v. Schnering and co-workers $Na[W_2O_2Br_6]$ [9] and by Perrin et al. the non-stoichiometric $Ag_{0.74}[W_2O_2Br_6]$ [10]. These compounds consist of WOI_3 analogue double-strands, which are negatively charged. Despite the compounds are of mixed valence with a mean oxidation level around 4.5 for W, the two tungsten atoms within an edge-sharing $WO_{4/2}X_6$ unit are in both cases crystallographically equivalent. The compounds can be classified as mixed valence compounds or as intercalates of tungsten oxide trihalides and metal cations. $Ag_{0.74}[W_2O_2Br_6]$ was found to have semi-conducting behaviour.

We have undertaken a systematic study of the reactivity of tungsten oxide trihalides $WOCl_3$ and $WOBr_3$ and could expand this structure family with various monovalent and divalent metal ions. In this first report we describe the structures and properties of the K^+, Tl^+, Pb^{2+} and Hg^{2+} representatives. Additionally we performed a structure analysis of $WOCl_3$ based on X-ray powder diffraction to confirm the WOI_3 structure type for this basic material and redetermined the structure of $Ag_{1-x}[W_2O_2Br_6]$ which was described originally with too low symmetry.

2. Experimental

2.1. Synthesis

$WOCl_4$ was prepared from Na_2WO_4 (Merck) and $SOCl_2$ (Merck) [11] and sublimed twice prior to use. All educts and reaction products were handled in an argon filled glove box. Ampoules were made of borosilicate glass and flame-dried in vacuo prior to use. TlCl, KCl and $PbCl_2$ were dried by heating at 450 K in vacuo. Tetrahydrofurane was dried by distillation from molecular sieve which was freshly dried in vacuo at 520 K.

$WOCl_3$ was prepared by reduction of $WOCl_4$ with Al powder (Riedel-de Häen) [12] as a green microcrystalline powder, which readily turns blue on contact to humid air. EDX analyses showed an Al content of up to 10 mol% in the products of different batches.

$WOBr_3$ was prepared from W (Merck), WO_3 (Fluka) and Br_2 (Merck) as described in Ref. [6].

$Tl_{0.98}[W_2O_2Cl_6]$: 30 mg (0.25 mmol) dry TlCl (Aldrich, >99.9%) and 77 mg (0.25 mmol) $WOCl_3$ were grinded and filled in a glass ampoule of 10 cm length and 1.4 cm diameter. The ampoule was sealed and placed in an horizontal tube furnace which was heated to 573 K. Within 2 days, long bluish-black needles with a metallic luster were obtained.

$K_{0.84}[W_2O_2Cl_6]$: 0.5 mmol (37 mg) dry KCl (Merck, 99.9%) and 0.5 mmol $WOCl_3$ (153 mg) were grinded, pressed to a pellet of diameter 0.9 cm and put into glass ampoule (l = 8 cm, d = 1.2 cm). The ampoule was evacuated, sealed and placed in an horizontal tube furnace which was heated to 623 K. After 4 days, the ampoule was removed of the furnace for assessment and afterwards heated again for 14 days at 648 K. Long bluish black needles were grown on the surface of the pellet. An EDX analysis of several different crystals showed a K:W ratio of 0.80(5):2 and no variation of the potassium content along the needle axes could be detected. The pellet itself consisted of about 2/3 of $K_{0.8}[W_2O_2Cl_6]$ and about 1/3 of $K_2[WOCl_5]$, according to X-ray powder diffractometry.

$Pb_{0.55}[W_2O_2Cl_6]$: 70 mg (0.25 mmol) dry $PbCl_2$ and 153 mg (0.5 mmol) $WOCl_3$ were grinded, pressed to a pellet of diameter 0.6 cm and put into a glass ampoule (l = 5 cm, $\varnothing$ = 1.0 cm). The ampoule was evacuated, sealed and placed in a horizontal tube furnace which was heated to 623 K. After 6 days, the product was obtained as black

lustrous needles. EDX analyses on four selected crystals showed a constant Pb:W ratio of 0.45(2):2.

$Hg_{0.55}[W_2O_2Cl_6]$: 536 mg Hg (Heraeus, 99.999%) (2.7 mmol) and 1436 mg $WOCl_4$ (4.2 mmol), were filled into an ampoule of 15 cm length and 1.8 cm diameter which was sealed and placed in a horizontal tube furnace which was heated to a temperature of 633 K. After 4 days the product was obtained as black lustrous needles, which were deposited in the colder end of the ampoule. The black crystals were formed as agglomerates with colourless $HgCl_2$ which was removed by repeated washing with dry THF under an argon atmosphere. This washing process had no detectable disadvantageous effects on the crystals of the product. EDX measurements gave a Hg:W-ratio of 0.53(6):2.

$Ag_{0.8}[W_2O_2Br_6]$: 24 mg (0.22 mmol) Ag powder (synthesized by reduction of a $AgNO_3$ solution with hydrazine) and 230 mg (0.52 mmol) $WOBr_3$ were grinded and filled into a quartz-glass ampoule (length = 10 cm, diameter = 1.0 cm). The ampoule was evacuated, sealed and placed in a horizontal tube furnace which was heated to 775 K. After 6 days bluish-black lustrous needle-shaped crystals were obtained. After manual separation, 70 mg of pure product resulted, which was used for magnetic measurements. EDX analysis on several crystals from different reaction batches showed a Ag:W-ratio of 0.75 ± 0.15:2.

To obtain crystals suitable for single crystal structure determination the ampoule was heated with 2 K/h to 975 K, kept for three days at this temperature and then at a temperature of 1075 K for another 3 days and finally at 1150 K for a period of 4 weeks. After rapid cooling to ambient temperature of 100 K/h only few but well crystallized needles were obtained that were used for the structure analysis.

2.2. X-ray powder diffraction structure analysis of $WOCl_3$

$WOCl_3$, synthesized from $WOCl_4$ and Al as described above, was filled in a thin walled glass capillary of 0.3 mm diameter, which was sealed. The diffraction data were collected with a Stoe StadiP diffractometer equipped with a linear position sensitive detector (PSD) in Debye-Scherrer geometry using Cu$K\alpha_1$ radiation ($\lambda = 1.540598$ Å). The d spacings were corrected against silicon ($a = 5.43088(4)$ Å) as an external standard. The diffractogram could be indexed according to the values given by Crouch et al. [6]. Nine broad, weak reflections (max. relative intensity < 0.7%) could not be indexed with the lattice parameters of $WOCl_3$ nor assigned to any known phase in the system W/O/Cl/Al. The structure model used was that of WOI_3 with the space group $P4_2/mnm$. The Rietveld refinement of the X-ray data was performed with the program GSAS [13,14]. For the obscure weak reflections, the corresponding measurement ranges were excluded (see Table 1). A March-Dollase [15] preferred orientation correction was applied (0 0 1 axis, ratio = 1.18). For absorption correction, a value of $\mu r = 1.8$ was chosen. The recorded and the calculated diffractogram are given in Fig. 1 together with the difference plot. Using the structural parameters of $NbOCl_3$ (space group $P\bar{4}2_1m$) as starting model for the refinement, the initial agreement between measured and calculated intensities was much poorer than in the case of WOI_3. In the course of the refinement, the W–W distance shortened from 3.84 to 3.00 Å and the W_2Cl_6 units became virtually planar, so that the WOI_3 type structure model gained further confirmation. Crystallographic data and details of the structure analyses are given in Table 1, the positional parameters are given in Table 4.

Table 1
Crystallographic data and details of the structure refinement for $WOCl_3$

Formula	$WOCl_3$
Crystal system; Space group	Tetragonal, $P4_2/mnm$
Temperature/K	295(2)
Unit cell dimensions/Å	$a = 10.6856(6)$ $c = 3.8537(2)$
Unit cell volume/Å^3	440.02(7)
Number of formula units	4
Calculated density/g/cm^3	4.60
Radiation	Cu$K\alpha_1$; $\lambda = 1.540598$ Å, Ge(111) monochromator
Data collection range/°	$6.98 \leqslant 2\theta \leqslant 99.72$
Limiting indices	$0 \leqslant h \leqslant 13$, $0 \leqslant k \leqslant 9$; $0 \leqslant l \leqslant 4$
Step width/2θ°	0.02
Excluded regions/2θ°	8.28–8.56; 12.62–12.78; 13.70–14.58; 16.08–16.30; 16.84–17.10; 21.26–21.76; 23.00–23.22; 28.32–28.60
Number of remaining data points	4490
Preferred orientation correction	March-Dollase, 0 0 1 axis, ratio = 1.18
No. of reflections	146
No. of atomic parameters	18
Overall no. of parameters	57
Reliability factors	
R_p	0.045
R_{wp} [%]	0.060
D_{dw}	0.523
red. χ^2/GooF ($\sqrt{\chi^2}$)	1.701/1.30 (57 variables)

Standard deviations given in brackets refer to the last significant digit.

2.3. X-ray single crystal structure analyses

All crystals were mounted in thin-walled glass capillaries, which were sealed. Data were collected using a Enraf-Nonius-Kappa-CCD diffractometer using graphite monochromatized Mo$K\alpha$ radiation. Low temperature was maintained with a nitrogen-gas-flow cooling system (Oxford Cryosystems). Temperatures were calibrated with a micro-thermocouple mounted instead of a crystal. All crystals were measured at ambient temperature, the crystal of $Tl_{0.98}[W_2O_2Cl_6]$ was measured additionally at 210 and 140 K. Due to the high absorption coefficients and the anisotropic shape of the crystals a numerical absorption correction with the aid of the program HABITUS [16] was

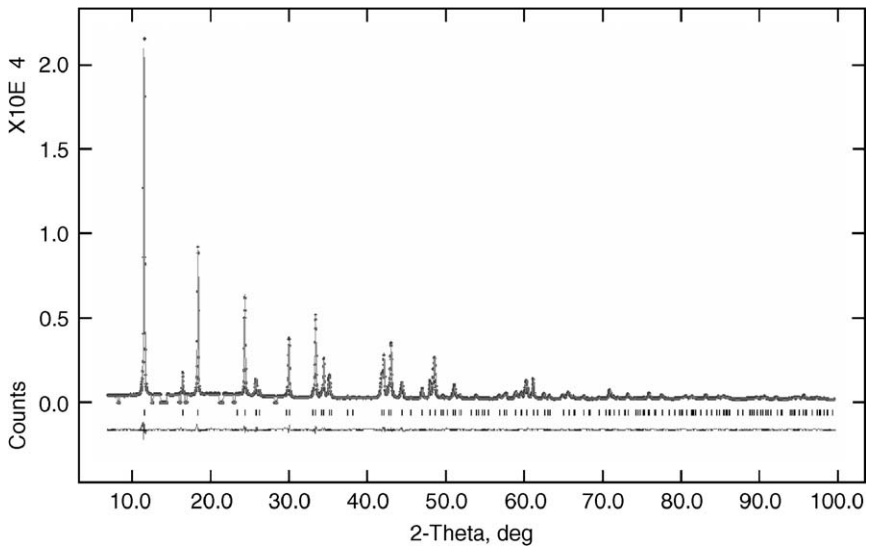

Fig. 1. X-ray powder diffractogram of $WOCl_3$ with measured (black dots) and calculated intensities (grey line), theoretical reflection positions (black bars) and difference curve (black line).

applied to all data sets. The optimization of the crystal shape was performed by minimalization of the reliability factor of averaging symmetry equivalent reflections. Structure models were obtained by direct methods and refined against F^2 using SHELX97 as implemented in the WINGX program package [17,18]. Tables 2 and 3 contain the crystallographic data and details of the structure analyses, positional parameters are given in Table 4 and selected bond lengths are given in Table 5.

2.4. Magnetic measurements

Magnetic susceptibilities were measured from 2 to 300 K with fields from 1 to 5 T with a PPMS (*Physical Property Measurement System*; Quantum Design). Samples were filled in gelatine capsules which were fixed in a gas tight plastic container at the sample holder. After *Zero Field Cooling* (ZFC) the appropriate field was applied and the susceptibilities were measured. The data were corrected for the susceptibility of the container material of the respective diamagnetic corrections [19]. For $Ag_{0.8}[W_2O_2Br_6]$ the diamagnetic correction amounts to $309 \times 10^{-6}\,cm^3/mol$ composed of $0.8Ag^+ = 19.2$, $2O^{2-} = 24$, $6Br^- = 216$, $W^{4+} = 26$, $W^{5+} = 19$, and for $Hg_{0.5}[W_2O_2Br_6]$ to $272 \times 10^{-6}\,cm^3/mol$ composed of $0.5Hg^{2+} = \sim 47$; $2O^{2-} = 24$; $6Cl^- = 156$; $W^{4+} = 26$; $W^{5+} = 19$, each given in terms of $-10^{-6}\,cm^3/mol$.

2.5. Electrical conductivity measurements

Conductivity measurements of $Hg_{0.6}[W_2O_2Cl_6]$ were performed on a pellet (13 mm diameter) of grinded crystals (Hg:W ratio 0.60(4):2, shown by EDX measurements) by the four-probe technique. The specific conductivity was found to be $0.053\,\Omega^{-1}\,cm^{-1}$ at room temperature and $0.016\,\Omega^{-1}\,cm^{-1}$ at 135 K. Due to the unknown influence of grain boundary effects, reliable values for the specific conductivity cannot be given. Attempts to obtain conductivity data from individual crystals were unsuccessful due to difficulties in contacting the extremely thin and mechanically sensitive needle shaped crystals.

3. Results and discussion

3.1. Syntheses

In principle compounds of the general formula $M_{1-x}[W_2O_2X_6]$ ($X = Cl$, Br) can be obtained by three different methods:

a. The thermal decomposition of $WOCl_3$ in the presence of the appropriate metal chloride:

$$3WOCl_3 + M^{n+}Cl_n \rightarrow (M^{n+})_{1/n}[W_2O_2Cl_6]^- + WOCl_4 \quad (M = K,\ Tl,\ Pb) \tag{1}$$

b. Reduction of $WOBr_3$ with the appropriate metal in its elemental state:

$$M + 2WOX_3 \rightarrow (M^{n+})_{1/n}[W_2O_2X_6]^- \quad (M = Ag) \tag{2}$$

c. Reduction of $WOCl_4$ by the appropriate metal in its elemental state:

$$2WOCl_4 + 3M \rightarrow (M^{n+})_{1/n}[W_2O_2Cl_6]^- + 2M^{n+}Cl_n \quad (M = Hg) \tag{3}$$

The success of the syntheses using $WOCl_3$ depends mainly on the way of its preparation. Only the product obtained by reduction of $WOCl_4$ with Al showed the desired reactivity. This material contains an amount of Al

Table 2
Crystallographic data and details of the structure refinement for $Tl_{0.98}[W_2O_2Cl_6]$ and $K_{0.84}[W_2O_2Cl_6]$

Formula		$Tl_{0.981(2)}[W_2O_2Cl_6]$		$K_{0.84(2)}[W_2O_2Cl_6]$
Crystal system; Space group		Monoclinic; $C2/m$		Monoclinic; $C2/m$
Temperature/K	295(2)	210(5)	140(5)	295(2)
Unit cell dimensions/Å	$a = 12.7050(4)$	$a = 12.6664(4)$	$a = 12.6377(6)$	$a = 12.812(3)$
	$b = 3.7797(1)$	$b = 3.7792(1)$	$b = 3.7791(2)$	$b = 3.7779(6)$
	$c = 10.5651(3)$	$c = 10.5273(4)$	$c = 10.5040(5)$	$c = 10.196(3)$
	$\beta = 107.840(1)$	$\beta = 107.656(1)$	$\beta = 107.530(2)$	$\beta = 107.422(8)$
Unit cell volume/Å^3	482.95(2)	480.19(3)	478.36(4)	470.9(2)
Number of formula units		2		2
Calculated density/g/cm^3	5.617	5.649	5.671	4.60
Data collection range/°	$4.0 \leqslant 2\theta \leqslant 55.0$	$3.4 \leqslant 2\theta \leqslant 54.9$	$6.8 \leqslant 2\theta \leqslant 61.1$	$6.7 \leqslant 2\theta \leqslant 54.99$
	$-16 \leqslant h \leqslant 16$	$-16 \leqslant h \leqslant 16$	$-17 \leqslant h \leqslant 17$	$-14 \leqslant h \leqslant 15$
Limiting indices	$-4 \leqslant k \leqslant 4$	$-4 \leqslant k \leqslant 4$	$-5 \leqslant k \leqslant 5$	$-4 \leqslant k \leqslant 3$
	$-13 \leqslant l \leqslant 13$	$-13 \leqslant l \leqslant 13$	$-14 \leqslant l \leqslant 14$	$-9 \leqslant l \leqslant 12$
Absorption correction	Numerical	Numerical	Numerical	Numerical
	$\mu = 42.01\,mm^{-1}$	$\mu = 42.25\,mm^{-1}$	$\mu = 42.41\,mm^{-1}$	$\mu = 26.43\,mm^{-1}$
Min./max. transmission	0.0656/0.7398	0.2699/0.7253	0.3084/0.7374	0.5766/0.9136
No. of reflections collected/unique	4912/637	5391/632	5629/779	1010/477
R_{int}	3.78	3.65	4.46	6.47
No. of parameters	37	37	37	37
Ratio data/parameters	17.2	17.1	21.1	12.0
Reliability factors				
$R(\|F\|)$	0.0116	0.0120	0.0199	0.0734
$R(\|F\|)$ $(n(F_o) > 4\sigma(F_o))$	0.0111(624)	0.0112 (615)	0.0188 (748)	0.0443 (359)
w$R(F^2)$	0.0256	0.0264	0.0385	0.0585
GooF	1.091	1.136	1.079	1.136
Final difference Fourier/e$^-$/Å^3	+0.76/−0.63	+0.61/−0.81	+1.71/−1.78	+1.75/−1.91

Standard deviations given in parentheses refer to the last significant digit.

Table 3
Crystallographic data and details of the structure refinement for $Pb_{0.55}[W_2O_2Cl_6]$, $Hg_{0.55}[W_2O_2Cl_6]$ and $Ag_{0.8}[W_2O_2Br_6]$

Formula	$Pb_{0.549(3)}[W_2O_2Cl_6]$	$Hg_{0.554(6)}[W_2O_2Cl_6]$	$Ag_{0.790(12)}[W_2O_2Br_6]$
Crystal system; Space group	Orthorhombic; $Immm$	Monoclinic; $C2/m$	Monoclinic; $C2/m$
Temperature/K	295(2)	295(2)	295(2)
Unit cell dimensions/Å	$a = 3.7659(1)$	$a = 12.8361(8)$	$a = 13.7338(10)$
	$b = 9.8975(4)$	$b = 3.7622(3)$	$b = 3.7769(3)$
	$c = 12.1332(6)$	$c = 10.2581(9)$	$c = 10.7954(9)$
		$\beta = 113.645(3)$	$\beta = 112.401(3)$
Unit cell volume/Å^3	452.2(2)	453.8(7)	517.71(7)
Number of formula units	2	2	2
Calculated density/g/cm^3	5.33	5.22	6.33
Data collection range/°	$6.7 \leqslant 2\theta \leqslant 58.2$	$6.54 \leqslant 2\theta \leqslant 54.96$	$6.2 \leqslant 2\theta \leqslant 60.2$
Limiting indices	$-4 \leqslant h \leqslant 4$	$-16 \leqslant h \leqslant 16$	$-19 \leqslant h \leqslant 19$
	$-13 \leqslant k \leqslant 13$	$-4 \leqslant k \leqslant 4$	$-5 \leqslant k \leqslant 5$
	$-16 \leqslant l \leqslant 16$	$-13 \leqslant l \leqslant 13$	$-15 \leqslant l \leqslant 15$
Absorption correction	Numerical	Numerical	Numerical
	$\mu = 37.32\,mm^{-1}$	$\mu = 36.38\,mm^{-1}$	$\mu = 46.78\,mm^{-1}$
min./max. transmission	0.1443/0.7343	0.0649/0.6485	0.0235/0.2255
No. of reflections collected/unique	4619/367	5243/601	7129/861
R_{int}	6.72	10.28	11.49
No. of parameters	24	38	39
Ratio data/parameters	15.3	15.8	22.1
Reliability factors			
$R(\|F\|)$	0.0247	0.0445	0.0453
$R(\|F\|)$ $(n(F_o) > 4\sigma(F_o))$	0.0203 (334)	0.0363 (535)	0.0363 (791)
w$R(F^2)$	0.0399	0.0656	0.0767
GooF	1.080	1.127	1.133
Final difference Fourier/e$^-$/Å^3	+1.48/–1.32	+1.74/–1.83	+3.49/–1.94

Standard deviations given in parentheses refer to the last significant digit.

Table 4
Wyckoff positions, site symmetry, site occupation factors (SOF), positional coordinates, and equivalent isotropic displacement parameters $U_{eq}/Å^2$ of the atoms in the structures of $WOCl_3$ and the $M_{1-x}[W_2O_2X_6]$ compounds

Atom	Wyckoff position and site symmetry	SOF	x	y	z	$U_{iso}/Å^2$
$WOCl_3$						
W	4*f* *m*2*m*		0.09901(7)	0.09901(7)	0	0.0642(9)
O	4*g* *m*2*m*		0.0911(7)	0.0911(7)	1/2	0.041(8)
Cl(1)	4*g* *m*2*m*		0.1257(3)	−0.12572(3)	0	0.062(4)
Cl(2)	8*i* *m*		0.3140(3)	0.1017(4)	0	0.063(3)
$Tl_{0.981}[W_2O_2Cl_6]$ (295 K)						
W	4*i* *m*		0.00407(1)	0	0.13710(1)	0.00999(8)
O	4*i* *m*		0.0037(2)	1/2	0.1355(3)	0.0125(6)
Cl(1)	4*i* *m*		0.15825(8)	0	0.05251(9)	0.0150(2)
Cl(2)	4*i* *m*		0.14237(9)	0	0.34940(10)	0.0219(2)
Cl(3)	4*i* *m*		−0.12787(9)	0	0.25700(10)	0.0195(2)
Tl	2*d* 2/*m*	0.9832(14)	0	1/2	1/2	0.04445(15)
$K_{0.84}[W_2O_2Cl_6]$						
W	4*i* *m*		0.00376(7)	0	0.141521(8)	0.0136(3)
O	4*i* *m*		0.0033(11)	1/2	0.1391(12)	0.019(3)
Cl(1)	4*i* *m*		0.1570(4)	0	0.0543(5)	0.0180(12)
Cl(2)	4*i* *m*		0.1402(5)	0	0.3601(5)	0.0247(13)
Cl(3)	4*i* *m*		−0.1259(5)	0	0.2690(5)	0.0261(13)
K	2*d* 2/*m*	0.84(2)	0	1/2	1/2	0.035(4)
$Pb_{0.55}[W_2O_2Cl_6]$						
W	4*g* *m*2*m*		0	0.14332(3)	0	0.01159(17)
O	4*h* *m*2*m*		1/2	0.1435(6)	0	0.0124(13)
Cl(1)	4*i* *mm*2		0	0	0.15890(17)	0.0165(5)
Cl(2)	8*l* *m*		0	0.32237(16)	0.13281(13)	0.0209(4)
Pb	2*c* *mmm*	0.549(3)	1/2	1/2	0	0.0349(5)
$Hg_{0.55}[W_2O_2Cl_6]$						
W	4*i* *m*		0.07588(5)	0	0.14603(6)	0.01648(18)
O	4*i* *m*		0.0748(7)	1/2	0.1450(9)	0.0125(16)
Cl(1)	4*i* *m*		0.1275(3)	0	−0.0534(3)	0.0209(7)
Cl(2)	4*i* *m*		0.2763(3)	0	0.2833(4)	0.0296(8)
Cl(3)	4*i* *m*		0.0616(3)	0	0.3722(3)	0.0316(8)
Hg	4*i* *m*	0.277(3)	0.2679(2)	0	0.5317(2)	0.0404(9)
$Ag_{0.8}[W_2O_2Br_6]$						
W	4*i* *m*		0.07102(4)	0	0.14359(5)	0.01509(18)
O	4*i* *m*		0.0691(6)	1/2	0.1391(8)	0.0141(15)
Br(1)	4*i* *m*		0.12832(9)	0	−0.05410(12)	0.0193(3)
Br(2)	4*i* *m*		0.2683(1)	0	0.28041(14)	0.0275(3)
Br(3)	4*i* *m*		0.05329(12)	0	0.36871(13)	0.0290(3)
Ag	4*i* *m*	0.395(6)	0.2654(3)	0	0.5323(3)	0.0563(15)

Standard deviations given in parentheses refer to the last significant digit.

Table 5
Selected bond lengths/Å and *M*–*M* bond strengths in compounds with $[M_2O_2X_6]$ and $[M_2O_2X_6]^-$ strands (M = Nb, W; X = Cl, Br)

Compound	*M*–O	*M*–*X*(1)	*M*–*X*(1)′	*M*–*X*(2)	*M*–*X*(3) *M*–*X*(2)′	*M*–*M*	$\Delta d/d$ according to Eq. (4)
$WOCl_3$	1.9294(11)	2.399(5)	2.399(5)	2.288(5)	2.288(5)	2.990(4)	0.098
WOI_3 [5]	1.8831(6)	2.6975(12)	2.6975(12)	2.7300(13)	2.7300(13)	3.102(1)	0.192
$Tl_{0.98}[W_2O_2Cl_6]$	1.8899(1)	2.3892(10)	2.3947(10)	2.3882(10)	2.3908(10)	2.8670(3)	0.152
$K_{0.84}[W_2O_2Cl_6]$	1.8891(3)	2.386(6)	2.401(4)	2.385(4)	2.396(6)	2.8590(2)	0.155
$Pb_{0.55}[W_2O_2Cl_6]$	1.8830(1)	2.3933(17)	2.3933(17)	2.3952(16)	2.3952(16)	2.8370(7)	0.162
$Hg_{0.55}[W_2O_2Cl_6]$	1.8812(2)	2.390(3)	2.393(3)	2.387(3)	2.400(3)	2.8441(11)	0.159
$Ag_{0.8}[W_2O_2Br_6]$	1.8890(3)	2.5404(12)	2.5323(13)	2.5440(13)	2.5331(14)	2.9677(10)	0.173
$Na[W_2O_2Br_6]$ [9]	1.888(1)	2.537(2)	2.537(2)	2.525(2)	2.525(2)	2.9458(9)	0.177
$NbOCl_3$ [3]	1.758(3)/2.203(3)	2.545 (2)	2.545(2)	2.274(2)	2.274(2)	3.911(2)	–0.148

of some mol%. A laser ablation mass spectral analysis of one of the products ($K_{0.8}[W_2O_2Cl_6]$) showed that Al was not incorporated. $WOCl_3$ prepared and purified by chemical vapour transport [20] turned out to be unreactive in these reactions. Yields are generally low and do not exceed 10%. In all cases it was found to be advantageous to press the educts to a pellet after grinding. The main product is generally $WOCl_2$, formed by disproportionation of $WOCl_3$. The quaternary products usually grow as lustrous, black, needle-shaped crystals out of the pressed pellet. Yields are better when using $WOCl_4$ as a starting material according to method c yields. In the case of the mercury containing compound yields close to 100% could be obtained since volatile $HgCl_2$ is present in the gas phase which makes chemical transport possible and the desired product deposits on the cold end of the ampoule.

For the Tl containing compound a by-product could be identified. Together with the black needles of $Tl_{1-x}[W_2O_2Cl_6]$, the formation of yellow-brown crystals was observed. They were identified as $Tl_2[WOCl_5]$, which crystallizes in the cubic system in the space group $Fm\bar{3}m$ with the lattice constant $a = 9.7978(3)$ Å. The structure is isotypic to $Cs_2[NbOCl_5]$ [21] and adopts the K_2PtCl_6 type with the O atom and Cl atoms of the $[WOCl_5]^{2-}$ group disordered over all six positions of the coordination octahedron.

3.2. Crystal structure of $WOCl_3$

$WOCl_3$ is a fibrous material which causes problems on recording diffraction data. The long and extremely thin crystals of $WOCl_3$ obtained by chemical vapour transport are notoriously twinned and not suitable for single crystal studies. Even for powder diffraction purposes this $WOCl_3$ is not suitable since the fibres cannot be grinded. On filling in capillaries or other sample holders the crystals take a preferred orientation which seriously falsifies the diffraction diagrams. $WOCl_3$ obtained by reduction of $WOCl_4$ by Al forms a dark-green loose mass. This material crystallizes as fine needles which need not to be grinded. So we found this material to be suitable for powder diffraction work despite the fact that EDX analyses showed a certain Al content in the samples up to 10 mol%. The nature of this impurity is not clear. In the diffractogram no strong additional reflections were present, only some broad, weak reflections with intensities close to the background were observed and could be excluded from indexing and refinement.

$WOCl_3$ crystallizes in the space group $P4_2/mnm$ with the lattice constants $a = 10.6856(6)$ Å and $c = 3.8537(2)$ Å. The structure is isotypic to WOI_3 [5] and consists of pairs of edge-sharing WO_2Cl_4 octahedra, which are connected via oxygen bridges to form infinite strands $^{\infty}_{1}[W_2O_{4/2}Cl_4Cl_{2/2}]^-$ along the *c*-axis (Fig. 2). The tungsten atoms are in the pentavalent state and have the d^1 configuration. The W–W distance within the edge sharing octahedra was found to be 2.99 Å, which is about 0.9 Å shorter than in the d^0 configurated $NbOCl_3$. The tungsten atoms are placed in the mirror plane perpendicular to the *c*-axis together with the chlorine atoms, so planar W_2Cl_6 units result. All atoms were refined with anisotropic displacement factors. The displacement component of the W atom in direction of the *c*-axis does not show any unusual features which underlines that W actually is located in the mirror plane. The W–O–W bridges are equidistant but with an angle of 172.9(6)° not linear. In contrast the structure of $NbOCl_3$ contains polar strands: the niobium atoms are shifted out of the centres of the NbO_2Cl_4 octahedra towards one of the oxygen atoms, therefore the Nb···O–Nb bridges along the strands are of alternating lengths. The length of the *c*-axis of 3.95 Å corresponds to the distance Nb···O–Nb, and is about 0.1 Å longer than in $WOCl_3$.

The distance of the tungsten atoms to the terminal Cl atoms Cl(2) is 2.29 Å which is much shorter than the distance to the bridging atoms Cl(1) of 2.42 Å. Compared with $NbOCl_3$, the difference in the W–Cl bond lengths between terminal and bridging Cl atoms is slightly larger in the niobium compound [3]. Other significant differences in geometrical details in the structures of $NbOCl_3$ and $WOCl_3$ are present in the Cl–*M*–Cl angles. The angle

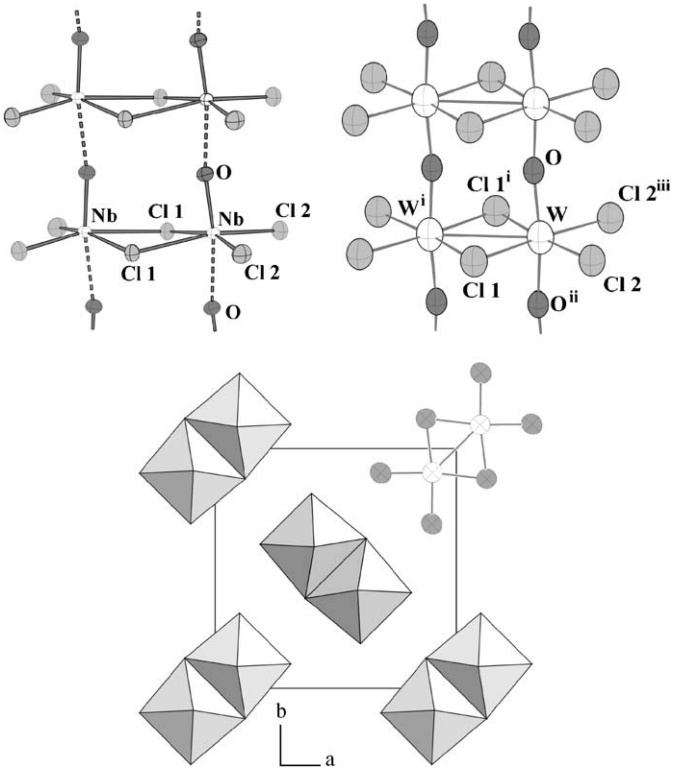

Fig. 2. Sections of the chains of edge-sharing $[M_2O_{4/2}Cl_6]$ groups in the structures of $NbOCl_3$ (left) and $WOCl_3$ (right). Thermal ellipsoides are drawn at the 50% probability level. Selected distances/Å and angles/°: W–W^{i} 2.992(2), W–O, W–O^{ii} 1.9305(7), W–Cl(1), W–Cl(1^{i}) 2.417(4), W–Cl(2), W–Cl(2^{ii}) 2.297(3), O–W–O^{ii}, W–O^{ii}–W^{ii} 172.9(6), Cl(1)–W–Cl(1^{i}) 103.53(14), Cl(2)–W–Cl(2^{ii}) 88.6(2), W–Cl(1)–W^{i} 76.47(14). Symmetry operations: i = $-x$, $-y$, z; ii = y, x, $-z$; iii = x, y, $-1+z$.

Cl(1)–W–Cl(1) is larger than 90° and the angle W–Cl(1)–W is smaller than 90°, while in the structure of $NbOCl_3$ the situation is vice versa. The same holds for the angle Cl(2)–W–Cl(2), which is contracted in case of $WOCl_3$ and enlarged in case of $NbOCl_3$. These comparisons indicate the presence of attractive *M–M* forces in $WOCl_3$ and repulsive *M–M* forces in $NbOCl_3$.[2]

Schäfer and v. Schnering proposed an empirical law for the interrelation between bond length and bond strength for complexes with *M–M* bonds [22]. The relative shift of the metal atoms out of the centres of the idealized edge sharing coordination octahedral determines the bond strength.

$$\Delta d/d = \frac{d(M-M)_{\text{ideal}} - d(M-M)_{\text{experimental}}}{d(M-M)_{\text{ideal}}}. \quad (4)$$

The "ideal" *M–M* distance is defined by $d(M-M)_{\text{ideal}} = d(M-X)\sqrt{2}$. The mean metal–halogen distance *M–X* for $WOCl_3$ is $\bar{d}(M\text{–}X) = 2.344$ Å and the experimental *M–M* distance is 2.99 Å. One obtains according to Eq. (4) a value for $\Delta d/d = +0.098$. The small but positive value indicates a weak bond between the two tungsten centres. For $NbOCl_3$ ($\bar{d}(M\text{–}X) = 2.410$ Å, $d(M\text{–}M) = 3.911$ Å) a value of $\Delta d/d = -0.148$ is obtained, indicating repulsive interactions. The magnetic properties of $WOCl_3$ has been measured by Crouch et al. [6]. The magnetic moment decreases from 0.53 B.M. at 323 K to 0.25 B.M. at 109 K and diminishes strongly to 0.07 B.M. when temperature is lowered to 79 K. The magnetic moment is much lower than expected for a single unpaired electron. $WOCl_3$ is probably an antiferromagnet with a Neél temperature above 323 K. At ambient temperature strong spin pairing and a W–W single bond is present.

The magnetic behaviour of WOI_3 is similar to that of $WOCl_3$ ($\mu_{\text{eff}} = 0.24$ B.M. at 583 K; 0.15 B.M. at 90 K), the W–W distance is 3.11 Å, the respective angles I_{terminal}–W–I_{terminal}, W–I_{bridge}–W and I_{bridge}–W–I_{bridge} are 84.5°, 70.2° and 109.8°. The distortions from rectangularity are stronger than in the structure of $WOCl_3$. It is unusual that the W–I_{terminal} bonds (2.730 Å) are longer than the W–I_{bridge} bonds (2.697 Å).

Another compound containing pentavalent tungsten and the structural feature of edge sharing double octahedra is WCl_5 [23] which is isotypic to α-$NbCl_5$ [24]. Despite the tungsten atoms have a d^1 configuration as in $WOCl_3$ no W–W bond is present indicated by a long W–W distance of 3.814 Å (α-$NbCl_5$: 3.962 and 3.969 Å, β-$NbCl_5$: 3.988 Å). This is in line with the paramagnetic behaviour and the magnetic moment, which was found to be $\mu_{\text{eff}} = 1.01\,\mu_B$ [25].

[2]It was noted by Cotton et al."…when two octahedra are joined without distortion, on a common face or edge, the metal atoms make a contact that is repulsive in the absence of *M–M* bond formation. Therefore, if no bond is formed, the repulsion should lead to changes that reflect the repulsive force: the (μ–*L*)–*M*–(μ–*L*) angles should decrease while the *M*–(μ–*L*)–*M* angles increase." [32].

3.3. Crystal structures of $Tl_{0.98}[W_2O_2Cl_6]$ and $K_{0.84}[W_2O_2Cl_6]$

$Tl_{0.98}[W_2O_2Cl_6]$ and $K_{0.84}[W_2O_2Cl_6]$ crystallize isotypically in the monoclinic space group *C*2/*m*. Table 2 contains the crystallographic data. The structures are made up of distorted WO_2Cl_4 octahedra which are connected via a common edge of two Cl atoms forming $W_2O_4Cl_6$ units. These units are connected via almost linear W–O–W bridges of the trans positioned O atoms to infinite $^1_\infty[W_2O_{4/2}Cl_6]$ strands running along the crystallographic *b*-axis. A twofold symmetry axis is running through the strands bisecting the common edge of the coordination octahedra. Since the W atoms and all six Cl atoms are located in mirror planes perpendicular to the *b*-axis the strands have 2/*m* symmetry but the deviation from the ideal *mmm* symmetry is small.

In the structure refinement of $Tl_{0.98}[W_2O_2Cl_6]$ the occupation factor of the Tl atom showed a small but significant under-occupation. The respective values of the occupation factors obtained from the low temperature data collected at 210 and 140 K were 0.9815(14) and 0.979(2), together with the value obtained at 295 K data an averaged value of 0.981(2) is obtained. Two additionally examined crystals from different reaction batches showed a full occupation but the overall data quality was much poorer. For $K_{0.84}[W_2O_2Cl_6]$ the under-occupation of the *K* site is much more pronounced. Electron beam stimulated X-ray emission spectroscopy on several different crystals showed a constant *K*:*W* ratio of 0.40(3):1 and no variation of this ratio along the needle axes of the crystals could be detected. The occupation factor of the *K* atom converged in the structure refinement to a value of 0.84(2) in good agreement with the EDX analysis.

The $^1_\infty[W_2O_{4/2}Cl_6]$ strands are negatively charged. One has to assume that the valence of the tungsten atoms balances the charges. Since the two W atoms in each strand are crystallographically equivalent by a twofold axis they are of mixed valence and only an averaged oxidation state for the W atoms can be given. So $Tl_{0.98}[W_2O_2Cl_6]$ contains formally $W^{+4.51}$ and $K_{0.84}[W_2O_2Cl_6]$ contains $W^{+4.58}$.

The $^1_\infty[W_2O_{4/2}Cl_6]$ substructure in both compounds is equivalent to the double strands in the structure of $WOCl_3$ but some significant bond length differences are present. Both, the W–W and the W–O bond are shortened by 0.1 and 0.04 Å indicating a stronger W–W bond in the quaternary compounds. The bonds between the tungsten atoms and the terminal chlorine Cl(2) and Cl(3) atoms are elongated by 0.1 Å as a consequence of the electrostatic potential of the Tl^+ and K^+ cations which influence only these Cl atoms. The Tl^+ and K^+ cations are coordinated by eight terminal Cl(2) and Cl(3) atoms in form of a distorted cube. The respective distances are for $Tl_{0.98}[W_2O_2Cl_6]$ $4 \times 3.3375(9)$ Å (Cl(2)) and $4 \times 3.2010(9)$ (Cl(3)) Å, for $K_{0.84}[W_2O_2Cl_6]$ $4 \times 3.219(5)$ Å (Cl(2)) and $4 \times 3.073(4)$ (Cl(3)) Å. The cations are located between the $^1_\infty[W_2O_{4/2}Cl_6]$ strands and connect the strands to layers in

the *b*–*c* plane (Fig. 3). The ionic radius of K^+ (1.65 Å) is slightly smaller than the radius of Tl^+ (1.73 Å) [26]. The lattice constant *b*, which corresponds to the direction of the one-dimensional $W_2O_{4/2}Cl_6$ strands, has the same length in both compounds. The smaller size of the K^+ ion leads to a significant shortening of the *c*-axis, which represents the direction perpendicular to the strands, by 3.5% with respect to the Tl containing compound.

The thermal motion of the thallium atom in the structure of $Tl_{0.98}[W_2O_2Cl_6]$ determined on the basis of diffraction data collected at ambient temperature is relatively large as can be seen by a voluminous displacement ellipsoid, which has its strongest elongation perpendicular to the layers (Fig. 3). We determined the crystal structure additionally at 210 and 140 K, but no phase transition or ordering of the Tl atom on closely neighboured sites was observed. A comparison of the lattice constants shows that the *b*-axis is almost invariant on lowering the temperature while the *a*- and *c*-axes each shrink by about 0.5% between 295 and 140 K. Fig. 4 shows the temperature dependence of the coefficients of the principal axes *R*(*i*) of the thermal displacement of the Tl atom in the structure of $Tl_{0.98}[W_2O_2Cl_6]$. While the components *R*(2) and *R*(3) can be extrapolated linearly to values of about zero at 0 K and thus indicate regular thermal behaviour, the component *R*(1), pointing mainly along the *a*-axis, shows a non-linear dependence on temperature, possibly caused by anharmonic vibration contributions.

3.4. Crystal structure of $Pb_{0.55}[W_2O_2Cl_6]$

$Pb_{0.55}[W_2O_2Cl_6]$ crystallizes in the orthorhombic space group *Immm* and is isostructural to $Na[W_2O_2Br_6]$ [10]. The structure refinement showed the site of the Pb atom to be under-occupied with a factor of 0.549(3), which is in good agreement with the Pb:W ratio of 0.45(2):2 obtained by EDX analysis. The structure contains $^1_\infty[W_2O_{4/2}Cl_6]^-$ strands connected by Pb^{2+} ions to layers in the *a*–*b* plane (Fig. 3). Due to the orthorhombic symmetry the $W_2O_{4/2}Cl_6$ double octahedra have *mmm* symmetry with the consequence that the two different terminal Cl atoms in the structures of Tl and K analogue are here symmetrically equivalent. The W–O–W bridges are almost linear. The Pb atoms are coordinated by eight Cl atoms. The coordination

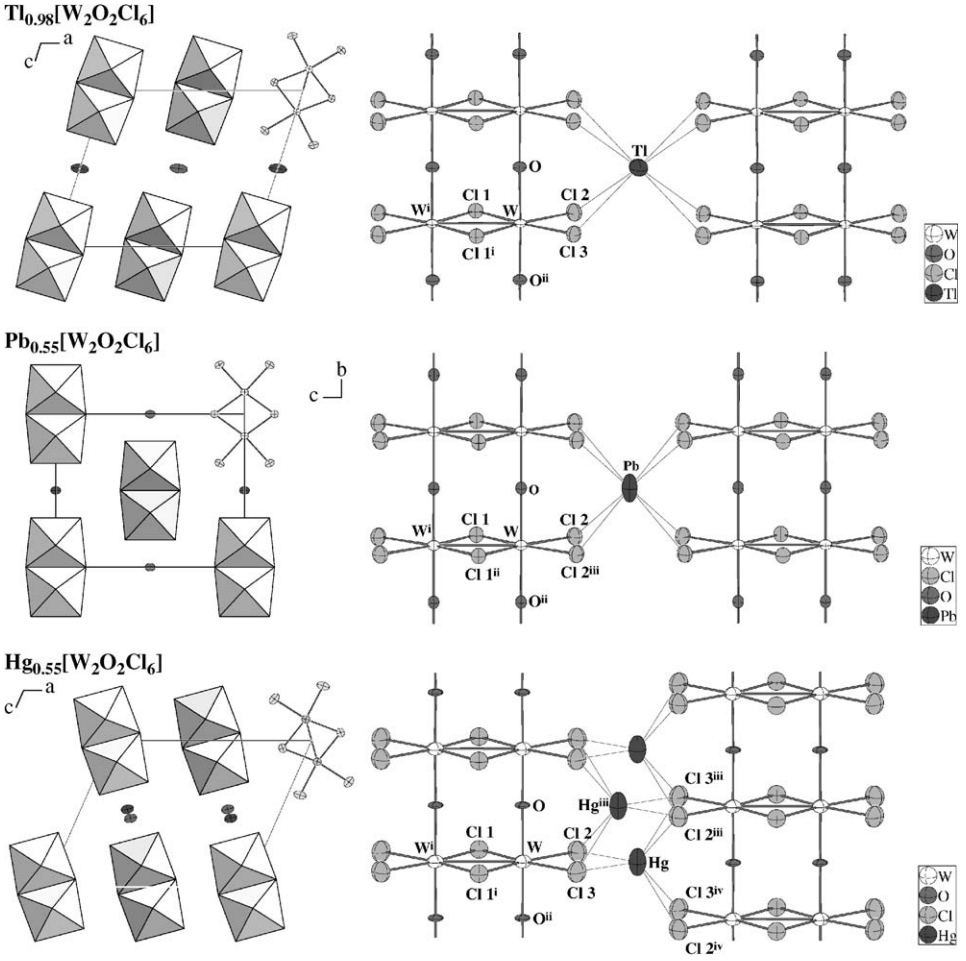

Fig. 3. The crystal structures of $Tl_{0.98}[W_2O_2Cl_6]$, $Pb_{0.55}[W_2O_2Cl_6]$ and $Hg_{0.55}[W_2O_2Cl_6]$, each depicted in a view along the $W_2O_2Cl_6$ strands (left) and sections of two neighboured strands showing the coordination of the cations (right). The displacement ellipsoids represent a probability level of the atoms of 70%.

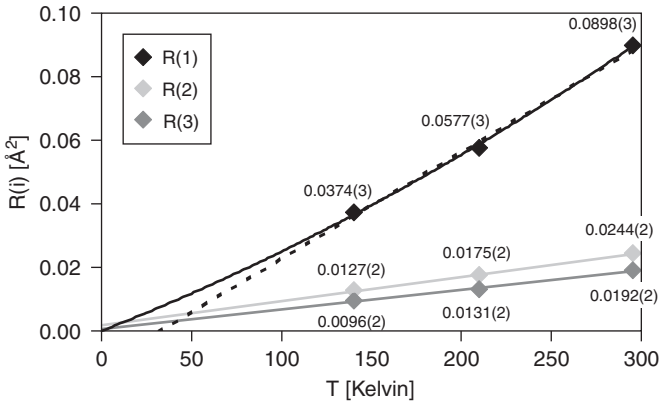

Fig. 4. Temperature dependence of the principal axes $R(i)/\text{Å}^2$ of the thermal displacement of the Tl atom in the structure of $Tl_{0.98}[W_2O_2Cl_6]$. The displacement coefficients of the components $R(2)$ and $R(3)$ can be extrapolated linearly to values close to zero at 0 K, while the coefficients of the component $R(1)$ can only be extrapolated to zero at 0 K assuming a non-linear function. A linear extrapolation is also drawn with a dotted line.

polyhedron has *mmm* symmetry and represents an only slightly distorted cube with eight equal Pb–Cl distances of 3.039(1) Å. A cube-shaped coordination environment is rarely found for halogeno plumbates and has been described only for PbF_2 [27]. With an occupation factor of 0.55 approximately every second Pb site is occupied giving the W atoms the oxidation number +4.45. Since the Pb ions carry two charges it is very unlikely that direct neighboured sites are occupied by Pb^{2+} with a distance of only 3.766 Å (the length of the *a*-axis). Thus, an alternating occupation of every second site is most probable. The superstructure reflections one can expect from this occupation were not observed in the diffraction diagrams. What can be understood by the assumption is that within every column of face sharing $PbCl_8$ cubes along the *a*-axis ordering is present but there is no coherence between these columns which are widely separated in the crystal.

3.5. Crystal structure of $Hg_{0.55}[W_2O_2Cl_6]$

$Hg_{0.55}[W_2O_2Cl_6]$ belongs to the monoclinic system and crystallizes in the space group $C2/m$. The basic building blocks in this structure are the one-dimensional $^1_\infty[W_2O_{4/2}Cl_6]$ strands and Hg^{2+} ions coordinated by the terminal Cl atoms of the negatively charged $W_2O_{4/2}Cl_6$ groups. The occupation factor of the Hg atom refined to 0.277(3) which is in excellent agreement with the Hg:W ratio of 0.53(6):2 found by EDX analysis. The oxidation state +4.45 for the W atoms is identical to the Pb containing compound. A profound structural difference exists to the monoclinically crystallizing congeners $Tl_{0.98}[W_2O_2Cl_6]$ and $K_{0.84}[W_2O_2Cl_6]$. Neighboured strands which are bound together by Hg ions to a layer are not located at the same height with respect to the W_2Cl_6 plane as observed for the Tl and K containing compounds but are alternating shifted in the direction of the strands by one W–O unit (Fig. 3). This strongly influences the coordination environment of the Hg atoms which do not have a cuboidal but rather a trigonal-prismatic coordination by six Cl atoms. The Hg–Cl distances (2.492(6), 2.594(5), $2\times2.752(4)$, $2\times2.885(4)$ Å) are separated in two groups of two short and four longer weak bonds indicating the distortion of the trigonal prism. Due to the low occupation factor of the Hg site only about one quarter of the Hg sites are actually occupied. The centres of gravity of neighboured trigonal prisms are only 1.983 Å apart. So it is impossible that directly neighboured positions are occupied by Hg^{2+} ions. Also the presence of Hg(I) can be ruled out. Since the distances between the Hg positions are shorter than the Hg–Hg distance in Hg_2^{2+} these dumb-bells cannot fit into the cavities and no Hg_2^{2+} molecules are present in the structure.

3.6. Crystal structure of $Ag_{0.8}[W_2O_2Br_6]$

$Ag_{0.74}[W_2O_2Br_6]$ was reported in 1998 by Perrin et al. to crystallize in the triclinic space group $P\bar{1}$ [11]. The application of the transformation (120, 100, $\bar{1}\bar{1}\bar{1}$) converts the reported cell to a monoclinic cell with the lattice constants $a=13.696$; $b=3.766$; $c=10.769$ Å; $\alpha=90.111°$; $\beta=112.445°$; $\gamma=89.963°$. This cell is perfectly in line with the monoclinic crystallizing compounds reported in this work. Additionally, a search for missing symmetry showed that the symmetry of the arrangement of the atoms in the transformed cell belongs to the space group $C2/m$ with very small deviations. So we redetermined the crystal structure and found that $Ag_{1-x}[W_2O_2Br_6]$ in fact belongs to the monoclinic system. The structure is isotypic to $Hg_{0.55}[W_2O_2Cl_6]$ and contains $^1_\infty[W_2O_{4/2}Br_6]$ strands which are isostructural to the Cl containing strands except the significant longer W–W bond of 2.968 Å, which corresponds to the W–W bond in $Na[W_2O_2Br_6]$ (2.946 Å [10]) but is shorter than the W–W bond in WOI_3 (3.103 Å [5]). The occupation factor of the Ag atom refined to 0.395(6) which is in good agreement with the Ag:W ratio found by EDX analyses of averaged 0.75:2.

3.7. Magnetic properties of $Ag_{0.8}[W_2O_2Br_6]$ and $Hg_{0.55}[W_2O_2Cl_6]$

Crystals of $Ag_{0.8}[W_2O_2Br_6]$ were measured applying three magnetic fields (1, 3 and 5 T). The 3 and 5 T data are nearly identical. Because of the slight field dependence, in Fig. 5 the 5 T data are represented. The reason of the slight field dependence is probably a small ferromagnetic impurity. Crystals of $Hg_{0.55}[W_2O_2Cl_6]$ were measured only at 1 T, therefore a field dependence is not known. No Curie or Curie–Weiss type paramagnetism is observed. Instead the molar susceptibilities are actually temperature independent. The observed temperature independent Pauli paramagnetism for both compounds is small and varies only slightly around $300\times10^{-6}\,\text{cm}^3\,\text{mol}^{-1}$ but is obviously

present. Even if the estimation of the diamagnetic increments was largely erroneous, the molar susceptibilities are staying positive.

3.8. Electrical conductivity of $Hg_{0.55}[W_2O_2Cl_6]$

The conductivity of a pressed powder sample of $Hg_{0.55}[W_2O_2Cl_6]$ obtained by a four-probe measurement applying direct current was $0.053\,\Omega^{-1}\,cm^{-1}$ at room temperature and $0.016\,\Omega^{-1}\,cm^{-1}$ at 135 K (Fig. 6). Reliable specific conductivity values cannot be given since the contribution of grain boundary effects on the resistance of the sample is unknown. Sintering of the pellet was not possible due to the temperature sensitivity of the compound.

An Arrhenius plot of $-\ln(\sigma)$ against $1000/T$ (Fig. 6, inset) shows a temperature dependence for the activation energy of the conduction process. Between ambient temperature down to 235 K the conductivity linearly decreases with temperature and an activation energy of 0.03 eV is obtained. At lower temperatures, the compound shows a diminishing gap which is typical for a variable range hopping (VRH) mechanism of the conductivity. Probably the conductivity occurs only along the one-dimensional strands. The percolation threshold for such a system is 100%, so all bonds in the strands have to be intact for showing the "theoretical"—probably metallic—conductivity. Since the measurement was done on a pellet of grinded crystals disrupting of the strands and lattice distortions as a result of mechanical bending of the crystals leads to an activation energy for the conduction process to appear. So a final decision whether the conductivity is semi-conducting or metallic cannot be made. Similar effects were observed in case of the Krogmann's salts [28].

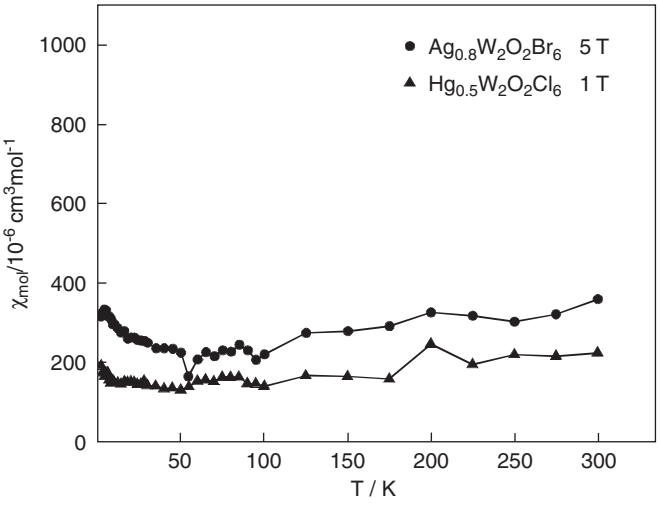

Fig. 5. Temperature dependence of the molar susceptibilities of $Ag_{0.8}[W_2O_2Br_6]$ and $Hg_{0.55}[W_2O_2Cl_6]$ in an external magnetic field of $H_0 = 5$ and 1 T, respectively.

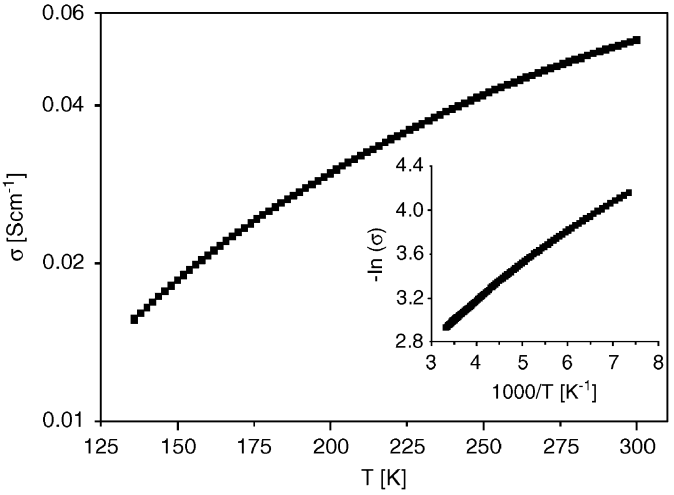

Fig. 6. Temperature dependence of the electrical conductivity for $Hg_{0.55}[W_2O_2Cl_6]$ in the temperature range 295–135 K. From the linear part of the Arrhenius plot (inset) an activation energy of 0.03 eV is obtained.

4. Conclusion

Tungsten oxide trihalides $WOCl_3$ and $WOBr_3$ show a particular reactivity to form non-stoichiometric quaternary compounds $M_{1-x}[W_2O_2X_6]$ with monovalent and divalent cations M. The structures of the respective compounds with $M = Na^+$ [10], Ag^+ [11], K^+, Tl^+, Pb^{2+} and Hg^{2+} are closely related despite they are not isotypic and show specific differences which are mainly triggered by the coordination demands of the cations. As a common structural feature the one-dimensional strands $^1_\infty[W_2O_{4/2}X_4X_{2/2}]$ from which $WOCl_3$ and $WOBr_3$ [29] are made up are present in all structures. A different relative arrangement of these strands is present and makes the structures of Tl^+/K^+ different from those of Na^+/Pb^{2+} and of Hg^{2+}/Ag^+. A short W–W bond is another common feature, shorter than the bond in $WOCl_3$. The application of Eq. (4) to all representatives shows clearly that a W–W bond is present with an increment $\Delta d/d$ two times higher in comparison to $WOCl_3$ (Table 5) [30]. The compounds are all of mixed valence, the tungsten atoms having an oxidation state between +4 and +5. Since the two W atoms of the dimeric units are in all cases crystallographically identical, a Robin-Day class-III mixed-valence [31] has to be assumed with no barrier to electron transfer between the two centres. The partial reduction of W(V) to the mixed valence (IV/V) state contracts significantly the W–O bonds along the strands from 1.93 Å in $WOCl_3$ to 1.88 Å. Since no paramagnetism was detected, one has to assume that the additional electrons are delocalized, probably along the –W–O–W– bonds. The high electrical conductivity and the very low energies for the thermal electron activation characterizes the compounds of the $M_{1-x}[W_2O_2X_6]$ family as one-dimensional semi-metals or even metals.

We started our work with the systematic exploration of the reactivity of $WOCl_3$. In a forthcoming article we will report on further investigations with special emphasis on the Cu containing representatives.

5. Supporting information

The crystallographic files in cif format have been deposited with the FIZ Karlsruhe under the CSD numbers 416393 for $WOCl_3$, 416392/416391/416390 for $Tl_{0.98}[W_2O_2Cl_6]$ at 293/210/140 K, 416388 for $K_{0.84}[W_2O_2Cl_6]$, 416389 for $Pb_{0.55}[W_2O_2Cl_6]$, 416387 for $Hg_{0.55}[W_2O_2Cl_6]$, 416386 for $Ag_{08}[W_2O_2Br_6]$. The data may be obtained free of charge by contacting the FIZ Karlsruhe via Fax at Intl. +49 7247 808 666 or via E-mail at crysdata@fiz-karlsruhe.de.

References

[1] D.E. Sands, A. Zalkin, R.E. Elson, Acta Cryst. 12 (1959) 21–23.
[2] M.G.B. Drew, I.B. Tomkins, Acta Cryst. B 26 (1970) 1161–1165.
[3] M. Ströbele, H.-J. Meyer, Z. Anorg. Allg. Chem. 628 (2002) 488–491.
[4] J. Beck, J. Bordinhão, Z. Anorg. Allg. Chem. 631 (2005) 1261–1266.
[5] B. Krebs, C. Brendel, H. Schäfer, Z. Anorg. Allg. Chem. 553 (1987) 127–135.
[6] P.C. Crouch, G.W.A. Fowles, J.L. Frost, P.R. Marshall, R.A. Walton, J. Chem. Soc. A (1968) 1061–1064.
[7] J. Beck, Angew. Chem. 103 (1991) 1149–1151; J. Beck, Angew. Chem. Int. Ed. 30 (1991) 1128–1131.
[8] J. Beck, Chem. Ber. 128 (1995) 23–27.
[9] Y.-Q. Zheng, K. Peters, H.G. von Schnering, Z. Anorg. Allg. Chem. 624 (1998) 1415–1418.
[10] S. Imhaïne, C. Perrin, M. Sergent, Mat. Res. Bull. 33 (1998) 927–933.
[11] H.-J. Lunk, W. Petke, Z. Chem. 14 (1974) 365.
[12] G. Brauer, Handbuch der Präparativen Anorganischen Chemie, F. Enke-Verlag, Stuttgart, Germany, 1981.
[13] A.C. Larson, R.B. von Dreele, General Structure Analysis System (GSAS), Los Alamos National Laboratory Report LAUR 86-748, Los Alamos, USA, 2000.
[14] B.H. Toby, EXPGUI, a graphical user interface for GSAS, J. Appl. Cryst. 34 (2001) 210–221.
[15] W.A. Dollase, J. Appl. Crystallogr. 19 (1986) 267–272; A. March, Z. Kristallogr. 81 (1932) 285–297.
[16] W. Herrendorf, H. Bärnighausen, HABITUS, Program for the Numerical Absorption Correction, Universities of Karlsruhe and Gießen, Germany, 1993 (1997).
[17] G.M. Sheldrick, SHELX97 [Includes SHELXS97, SHELXL97, CIFTAB]—Programs for Crystal Structure Analysis (Release 97-2), Universität Göttingen, Germany, 1998.
[18] L.J. Farrugia, J. Appl. Crystallogr. 32 (1999) 837–838.
[19] A. Weiss, H. Witte, Magnetochemie, Verlag Chemie, Weinheim, Germany, 1973.
[20] J. Tillack, Inorg. Synth. 14 (1973) 109–122.
[21] D. Brown, J. Chem. Soc. (1964) 4944–4948.
[22] H. Schäfer, H.G.v. Schnering, Angew. Chem. 76 (1964) 833–868.
[23] F.A. Cotton, C.E. Rice, Acta Crystallogr. B 34 (1978) 2833–2834.
[24] W. Hönle, H.G. von Schnering, Z. Kristallogr. 191 (1990) 139–140; F.A. Cotton, P.A. Kibala, M. Matusz, R.B.W. Sandor, Acta Crystallogr. C 47 (1991) 2435–2437.
[25] B.J. Brisdon, D.A. Edwards, D.J. Machin, K.S. Murray, R.A. Walton, J. Chem. Soc. A (1967) 1825–1831.
[26] R.D. Shannon, Acta Crystallogr. A 32 (1976) 751–761.
[27] N.H. Kolderup, Mineral. Abstracts 3 (1924) 340.
[28] P. Würfel, H.D. Hausen, K. Krogmann, P. Stampel, Phys. Stat. Sol. (A) 10 (1972) 537–541.
[29] The crystal structure of $WOBr_3$ is not known in detail. The powder diffractogram is reported to have an intensity pattern closely related to that of $WOCl_3$ and can be indexed by a tetragonal cell with the lattice constants $a = 11.35$, $c = 3.82$ Å: P.C. Crouch, G.W.A. Fowles, I.B. Tomkins, R.A. Walton, J. Chem. Soc. (A) (1968) 1061–1064. It is thus very likely that $WOBr_3$ is isotypic to $WOCl_3$ and WOI_3.
[30] The significance of the bond strength increment $\Delta d/d$ is limited by the significant influence of the type of halogen atoms surrounding the W atoms. There is clear increase of $\Delta d/d$ in the series Cl–Br–I, so only compounds with the same sort of halogen should be compared.
[31] M.B. Robin, P. Day, Adv. Inorg. Chem. Radiochem. 10 (1967) 247–422.
[32] F.A. Cotton, D. deMarco, B.W.S. Kolthammer, R.A. Walton, Inorg. Chem. 20 (1981) 3048–3051.